Detrital Zircon Geochronology and Vitrinite Reflectance Analysis of the Cascadia Subduction Complex, Washington

Peter Mahony

Advisor: Mark Brandon
Second Reader: Alan Rooney

May 2, 2018

A Senior Thesis presented to the faculty of the Department of Geology and Natural Geology, Yale University, in partial fulfillment of the Bachelors Degree.

1. Abstract:

The Cascadia subduction zone, which presently spans some 1,300 km along the western continental margin of the Pacific Northwest, was initiated ~35 Ma ago. A subduction complex has grown above this subduction zone, due to convergence (30-40 km/Ma) and accretion of the ~2 km-thick sedimentary cover of the subducting offshore plate (Farallon/Juan de Fuca). The result has been a gradual uplift of the Pacific Northwest coast. The Olympic Mountains in Washington State was the first part of the Cascadia subduction complex to emerge above sea level and is the most deeply eroded part of the Cascadia subduction complex (Brandon et al. 1998). Thus, this region provides a unique opportunity to study the accretionary evolution of the Cascadia margin.

We present ~1,600 new U/Pb ages for detrital zircons from 16 sandstone samples collected from the Olympic Mountains, and ~4,250 fission-track (FT) zircon grain ages from 95 sandstone samples, generated in previous work. Some of the FT samples are reset, as a result of post-depositional heating to temperatures > 200° C. The unreset FT zircons and all of the U/Pb zircons (which are insensitive to thermal resetting) preserve ages that were set in the erosional source region where the zircons were derived. The youngest zircons in each sample were sourced in the coeval Cascade volcanic arc, and thus should have ages similar to the depositional age of the sandstone sample.

These proxy depositional ages are used to the test the accretionary interpretation of the Cascadia subduction complex. The ages in fact show a clear younging from east to west, consistent with the progressive accretion of trench-fill turbidites at the offshore trench, which has been the leading accretionary edge of the subduction complex.

We use vitrinite reflectance data from 120 locations collected by Park Snavely (USGS) to define at a regional scale the maximum temperature for the exposed bedrock. The highest values, ~250° C, are found in the center of the Olympics Mountains, and they mark the most deeply eroded part of subduction complex, to an estimated depth of ~12.5 km. Reset zircon FT ages in this area indicate that the exposed rocks cooled below ~240° C at ~10 Ma. This result is

consistent with long-term erosion within the thicker, more rearward part of the subduction complex.

2. Introduction:

The Olympic Subduction Complex (OSC) formed as material from the subducting Farallon and Juan de Fuca plates assimilated onto the North American plate. The extant Farallon Plate began subducting beneath North America approximately ~35 Ma ago initiating wedge formation (Vance et al. 1986, summarized in Brandon and Vance 1992). At the active subduction zone, sediments from the trench have been scraped off and added to the overriding North American plate. Successive sedimentary layers have accreted at the margin, either by entraining to the frontal edge of the accumulating wedge of sediments or by sticking to the bottom of it, known as underplating (Brandon 2004). As more sediments have been added the wedge has thickened vertically and emerged from the Pacific Ocean (Brandon 2004). Once subaerially exposed surface processes eroded the resistive upper layers, often referred to as the structural lid, and exposed the imbricated sedimentary core (Brandon 2004). By studying the OSC we may draw general conclusions on accretionary wedge formation that can then be extrapolated to other subduction complexes.

There are few age constraints on the heavily deformed layers of accumulated sediments in the OSC. Previous attempts to date the OSC have relied on relative dating with microfossils, isotope analysis of basalts, apatite (U-Th)/He ages, and fission track ages of detrital apatites and zircons (summarized in Brandon and Vance 1992; Roden et al. 1990; Rau 1964; Snavley and Macload 1974 and others). The lower temperature thermochronometers, such as (U-Th)/He and fission-track apatite ages, are good for estimating thermal histories, given their low closure temperatures, ~65° C and ~110° C, respectively, while zircon fission-track ages can preserve age information if the temperature remains less than ~200° C (summarized in Batt et al. 2001). However these methods do not record reliable age information for the heavily eroded terranes at the center of the Olympic Mountains (Brandon and Vance 1992, Roden et al. 1990). Relative dating with microfossils is challenging because the marine sediments in the Olympic Mountains did not retain a robust fossil record, and when present, the fossil record was fractured during accretion (Rau 1964, Tabor and Cady 1978a). In situ basalts are limited to the

margins of the Olympic Peninsula, and are often metamorphosed making K-Ar and Ar-Ar analysis imprecise (summarized in Brandon and Vance 1992). In the past zircon fission track ages have been used because zircons have a high thermal stability and local crystals contain sufficient Uranium to give a low relative error (~10%) (Brandon and Vance 1992). It is agreed that the age of the youngest zircons in a sample is a good approximation of the depositional age because transport time from coeval zircon sources in the Cascadia Volcanic front is not significant (Stewart and Brandon 2004). We also propose that the youngest sample age in a unit is also a general approximation of the age of deposition for the entire unit. This implies that the depositional environment was regionally consistent. However dating fission tracks is time consuming and at temperatures exceeding ~245° C zircon fission tracks are no longer a reliable chronometer, as the fission tracks anneal and the crystal thermally resets (Brandon and Vance 1992). Previous zircon FT studies by Brandon and Vance have found that zircons in the Olympic Mountains were likely reset because the distribution of ages is not indicative of a depositional environment, where crystals of multiple ages may be incorporated, but of a single cooling event (Brandon and Vance 1992). U/Pb dating by of detrital zircons by laser ablation is preferable because the daughter isotopes for the $^{206}Pb/^{238}U$ and $^{207}Pb/^{206}Pb$ system are retained at high temperatures, with ~900 ° C required to fully reset the age (Cherniak and Watson 2001). For this reason new detrital zircon U/Pb minimum ages will be compared with the previous fission track data to confine the depositional ages of the sedimentary formations of the OSC.

Herein, vitrinite reflectance data collected by Parker Snavely will also be analyzed to determine the maximum temperature of the different layers of the accretionary wedge. Vitrinite is a glassy component of metamorphosed organic material that becomes more reflective the more it's heated (summarized in Barker and Pawlewicz 1994). By analyzing the reflectivity of the vitrinite in a sample we can calculate the maximum temperature the sample experienced (Barker and Pawlewicz 1994). Currently the thermal history of the OSC is poorly confined because it is based on metamorphic facies minerals and fission-track closure ages (Batt et al. 2001). Metamorphic facies analysis is an imprecise indicator of

maximum temperature because metamorphic processes often are dependent on pressure and because samples are limited by the presence of diagnostic minerals that are not always present (Sweeney and Burnham 1990). Fission tracks as thermochronometers are also not ideal because they are imprecise and unreliable at higher temperatures. As the sediments are exhumed and cooled the zircon and apatite crystals in the sandstones stabilize at ~245° C (~13 km) and ~100° C (~5 km) respectively (Brandon and Vance 1992, Brandon et al. 1998). Once the crystal has cooled below its resetting temperature, damage from fission decay of Uranium is recorded as tracks in the crystal lattice, thus the crystal records when it crossed the closure threshold (summarized in Batt et al. 2001). The cooling path can then be determined by analyzing the relative fission track ages of apatite and zircons in a sample, however fission track analysis does a poor job of constraining the maximum temperature because the thermal maximum is only discretized into three groups >245° C, between 245° C and ~100° C, and <100° C (summarized in Batt et al. 2001). Additional analysis into the thermal history of the different sections of the wedge is valuable because it will help to define the pathway each layer took during accretion.

This paper will summarize the geologic context of the Olympic Subduction Complex to explain how the Olympic Mountains reached their present configuration. It will then outline the methodology used to produce the $^{206}Pb/^{238}U$ and $^{207}Pb/^{206}Pb$ ages, and maximum temperature constraints. Next it will summarize the results of the Mahony Brandon detrital zircon minimum ages and the Shnavley Vitrinite Reflectance data, comparing them to the Stewart Brandon Fission Track ages. The paper will conclude with a discussion of how the new age and thermal constraints compares with the current theory of wedge dynamics.

3. Geologic Overview:

Brandon and Vance contend that coastal wedge systems can be divided into 4 discrete tectonic elements: a resistive continent, a volcanic arc, a coastal range terrane and an accretionary wedge (Brandon and Vance 1992). The continent acts as a plow that the incoming sediments accumulate against, and while some deformation can be expected the continent is generally considered fixed (Brandon

2004). Moving coastward the next element is the volcanic arc. The volcanic arc is coeval to the subduction zone and forms as melts are emplaced as plutons and volcanic rocks (Sherrod and Smith 1989). Yet farther coastward is the Coastal Range terrane. This is the coastal region that when subduction began was located between the subducting plate and the volcanic arc. And the furthest outboard element is the accretionary wedge, which is composed of accreted sediments from the subducting plate (Brandon and Vance 1992).

In the Cascadia Subduction Complex all four elements are present. The North American plate, composed of Paleozoic and Mesozoic structures sutured to the continental margin during the Jurassic and Cretaceous, is the resistive continent (Monger et al. 1982, Brandon et al. 1988, summarized in Brandon and Vance 1992). The subduction related volcanic arc is the Cascade Volcanic front, composed of exposed subvolcanic plutons as well as active stratovolcanoes; including Mt. Lassen in Northern California and Mt Garibaldi in British Columbia (Sherrod and Smith 1989). The Cascade Volcanic arc has been mostly stationary, although geologic and paleomagnetic data suggests there has been internal deformation and rotation during the Cenozoic (Heller et al. 1987, Wells and Heller 1988, summarized in Brandon and Vance 1992). It should be noted that some suggest that the Cascade arc was predated by the Challis arc, however Challis volcanism likely peaked between 52 Ma and 42 Ma, which does not overlap with estimates for OSC wedge building (Armstrong 1978, Heller et al. 1987). The two most outboard elements, the coastal range terrane and the accretionary wedge, are present in the Olympic Mountains and have seen extensive deformation during wedge formation.

The stratigraphy of the Olympic Mountains is highly deformed with extensive accretion related folding and thrust faulting, resulting in dissimilar formations abutting one another (Tabor and Cady 1978b, Brandon and Vance 1992). The geology of the OSC can be divided into two sections; a Paleogene basalt formation on the Northern, Eastern, and Southern margins known as the Crescent Formation, and a younger Cenozoic sedimentary core (Brandon and Vance 1992).

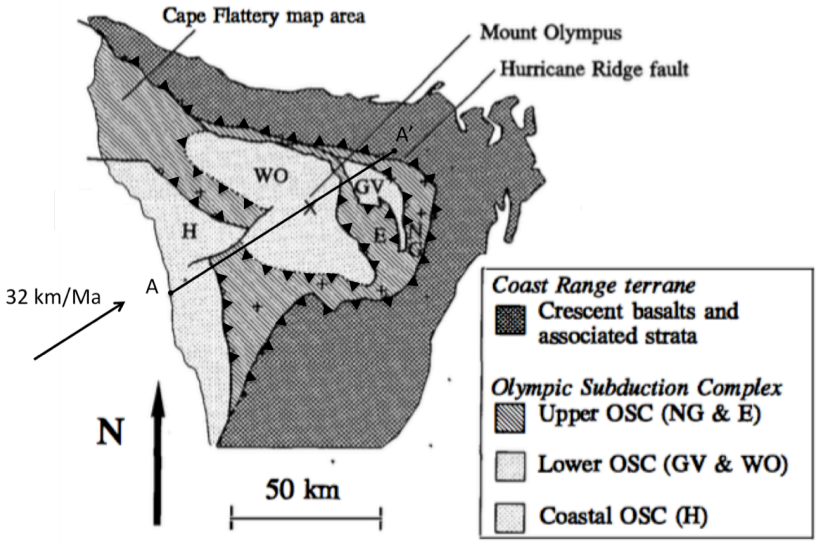

Figure 1: A-A' marks the cross section from the Kalaloch Lodge (A) to a point in the Coast Range terrane 100 km in the direction of plate (A). Location of Kalaloch Lodge (Pazzaglia and Brandon 2001) and asmuth angle from (McCaffery et al. 2013). Figure 2 is an approximate schematic of A-A'. The lithic assemblages are abbreviated with NG = Needles-Gray Wolf, E = Elwha, GV = Grand Valley, WO = Western Olympics, and H = Hoh; Adapted from Brandon and Vance 1992

3.1 Crescent Formation:

The Crescent formation is the Paleogene basalt formation on the periphery and is composed of feldspathic pillow basalts atop more massive basalt blocks (Tabor and Cady 1978a, Wells et al. 2014). Crosscutting the Crescent formation is Paleocene to Eocene dikes suggesting near-trench, or island arc volcanics (Tabor and Cady 1978a, Johnson 1984, Brandon and Vance 1992). The Crescent is a general stratigraphic unit of basalts that lie structurally above the younger sedimentary core at the Hurricane Ridge thrust fault (Tabor and Cady 1978a); the Crescent can be further subdivided based on different styles of deformation and paleo-rotation measurements (summarize in Brandon and Vance 1992, Siberling et al. 1987). The Crescent formation is not like the pre-tertiary formations on Vancouver Island or across the Puget Sound; it is more similar to uplifted oceanic crust or an entrained island chain (Johnson 1984, Brandon and Vance 1992). Brandon and Vance contend that the Crescent formation is part of the Coastal Range terrane (Brandon and Vance 1992). As the accretionary wedge encroached a section of marine sediment was incised and projected beneath the Crescent

formation roughly 33 Ma-17 Ma ago (Brandon and Vance 1992). Progressively more sedimentary layers have projected beneath the Crescent folding it upward until it was subaerialy exposed and eroded away leaving a heavily inclined stratigraphic column (Brandon and Vance 1992).

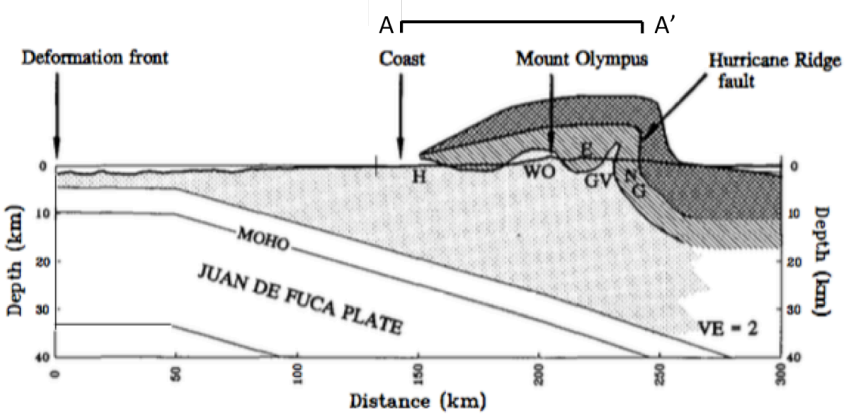

Figure 2: Schematic view of the the A-A' cross-section of the wedge depicting regional folding and nappe formation of the structural lid. Adapted From Brandon and Vance 1992

3.2 Sedimentary Core:

The sedimentary core is composed of imbricated assemblages of marine sandstone and mudstone with occasional inter-bedded lenses of early Paleogene pillow basalts that are more common near the Hurricane Ridge thrust fault (Tabor and Cady 1978b, Brandon and Calderwood 1990). The interior of the peninsula is internally faulted with friable layers closest to the subduction zone and progressively more thermally metamorphosed and resistive sediments as you move eastward deeper into the wedge (Tabor and Cady 1978b). The sedimentary core can be subdivided into five lithic assemblages from east to west: the Needles Gray Wolf, the Grand Valley, the Elwah, the Western Olympic, and the Hoh. Each of these sedimentary lithic assemblages are lenticular and separated by east-west thrust faults (Tabor and Cady 1978b; Heller et al. 1992). Brandon and Vance group these lithic assemblages into three structural units: the Upper OSC, the Lower OSC, and the Coastal OSC, based on their age, thermal history, and general stratigraphy (Brandon and Vance 1992). Each of the structural units defined by Brandon and Vance are coherent sections of incoming sediments from the wedge and record the

temperature and time history of their accretionary pathway (Brandon and Vance 1992, Batt et al. 2001).

3.2a Upper OSC:

Brandon and Vance refer to the Needles Gray Wolf, Elwah and several coastal assemblages collectively as the Upper OSC (Brandon and Vance 1992). The Upper OSC contains interbedded sandstone and limestone strata with Eocene to Oligocene marine microfossils, along with pillow basalts similar in age and composition to the overlying Crescent formation (Applegate and Brandon 1989, summarized in Brandon and Vance 1992). The Upper OSC does not contain diagnostic metamorphic facies minerals and is confined to between 90° and 250°C by fission track analysis (Frost 1980, Brandon et al. 1988, summarized in Brandon and Calderwood 1990).

The Upper OSC is interconnected with the Crescent formation based on the analogous basalt formations. Brandon and Vance contend that the Upper OSC was a western extension of the Coast Range terrane that was underthrust beneath the Crescent early in subduction (Brandon and Vance 1992). The Upper OSC is then considered to be part of the structural lid that was folded over Mount Olympus and largely eroded (Brandon and Vance 1992, Tabor and Cady 1978a)

3.2b Lower OSC:

Structurally below the Needles Gray Wolf and Elwah assemblages is what Brandon and Vance call the Lower OSC, containing the Grand Valley and Western Olympic lithic assemblages (Brandon and Vance 1992). The Lower OSC is composed of turbidites, thinly bedded mudstone mélanges, and clastic rocks likely transported to the trench by large-scale mass wasting events (Tabor and Cady 1978b, Brandon 1988, Brandon and Vance 1992). The Lower OSC features prehnite and pumpellyite facies minerals indicative of 240 to 245° C and a depth of ~12 km (Brandon and Calderwood 1990, summarized in Brandon and Vance 1992).

Brandon and Vance suggest that the Lower OSC accreted along the bottom of the wedge via underplating and was deeply buried resulting in reset zircons and higher metamorphic grade minerals (Brandon and Vance 1992).

3.2c Coastal OSC:

The Coastal OSC contains the Hoh assemblage. The Coastal OSC, like the Lower OSC, is composed of turbidites and thinly bedded mudstone mélanges with locally derived Miocene microfossils (Rau 1979), however instead of clastic rocks there are basalt blocks and instead of prehnite and pumpellyite there is zeolite-facies laumonite (Tabor and Cady 1978b, Brandon and Calderwood 1990).

The Coastal OSC was likely never deeply buried as the zeolite minerals indicate only low-grade metamorphism and FT samples are generally unreset. For this reason Brandon and Vance suggest that the Coastal OSC accreted along the frontal edge of the wedge (Brandon and Vance 1992).

4. Methodology:

4.1 U/Pb Zircon:

16 samples of medium to large grain sandstones were collected for $^{206}Pb/^{238}U$ and $^{207}Pb/^{206}Pb$ dating by LA-ICP-MS. The coastal, lower, and upper OSC units are represented in the analyzed samples with a focus on the most highly exhumed central massif near Mount Olympus. Efforts were taken to collect samples near sites previously dated by Brandon and Stewart using zircon fission tracks for comparison. Highway 1 circumnavigates the Olympic Peninsula and aided access to exposed sights on the periphery of the complex, while arterial logging and recreational roads provided access to samples in the national forest. Samples from the central massif and the slope of Mt. Anderson in the Elwha assemblage were reached via the extensive trail system provided by the US National Park Service.

The samples were then sent to Zirchron, LLC located in Tuscon, AZ where the zircon crystals were separated using the traditional mineral separation techniques from Armstrong 1986. The sandstones were first crushed to liberate the mineral grains. Then a Ro-Tap machine using 34-sized mesh sieved the mineral grains to remove the largest grains that would otherwise distort attempts to separate crystals based on density. The crystals ejected from the Ro-Tap and sieve were then sent for density separation to remove the lighter minerals.

A three-step density separation technique was used to isolate the dense zircons from lighter grains. First the lightest constituents, quartz and dust, were removed by a Wilfley Table. In the Wilfley Table the grains are suspended in water and shaken, causing the heaviest materials to sink but the lighter materials to remain suspended. The light minerals were removed and the water was drained leaving only dense crystals. Before additional density separation could take place, clay, carbonate, and magnetic minerals were removed. The dense crystals from the Wilfley Table were soaked in hydrogen peroxide solution overnight to remove clay minerals, and then soaked for another day in acetic acid solution to remove carbonate minerals. Magnetic grains were removed using a Frantz magnetic separator. The remaining crystals were then subjected to heavy liquid separation using lithium heteropolytungstate (LST) [density ~2.8 g/mL]. The crystals were mixed into the LST and allowed to settle; any grains that didn't sink were removed from the surface. A second heavy liquid separation using methylene iodide (MeI) [density ~3.3 g/mL] removed lingering apatite. In the processed samples the final heavy liquid separation yielded sufficient zircon crystals with negligible unintended pyrite. The isolated zircon crystals were then sent to University of California at Santa Cruz for LA-ICP-MS analysis in Dr. Jeremy Hourigan's laboratory.

At Jeremy Hourigan's laboratory the zircon samples were arbitrarily separated into two groups and placed on an epoxy mount for analysis. The zircon samples were first removed from their packaging, placed on a piece of double sided tape, and then transferred to a circular 1" form. The grains were organized into circular groups based on their sample, with additional groups featuring age-diagnostic standards. The form was then filled with Struer Epofix and allowed to cure. Excess epoxy was removed from the solid mounts using a lathe and 1500-grit sandpaper. The mounts were polished using a lap wheel with progressively finer Struers polishing compounds (summary of zircon separation and preparation based extensively on Sniderman 2013 and Armstrong 1986).

The mounts were then washed and laser ablation sites picked. 1% HNO_3 solution was used to chemically polish the surface of the mounts and pure water was used to rinse any remaining residue before the mounts were placed in the

Helex-2 volume cell. Approximately 100 laser ablation sites were picked per sample making sure to avoiding fluid inclusions or any remaining pyrite crystals. In two days of testing, one for each mount, the Helix-2 LA-ICP-MA collected isotope measurements from 1,581 sample zircons. For each zircon crystal the collector hood was removed before the laser was turned on to establish an average background ^{204}Pb measurement that would be subtracted from the on-peak signal. Laser ablation and on-peak collection lasted for 30 seconds. At the beginning and end of each testing session a block of standard crystals were analyzed, and throughout the testing period every 7th zircon analyzed was a standard.

The isotope data was then reduced to remove the bias from downhole elemental fractionation using Iolite based on industry standards outlined in Paton et al. 2010 and under the guidance of Jeremy Hourigan (Paton et al. 2010). Samples that displayed noticeable ^{204}Pb anomalies indicative of fluid inclusions or high radiation damage were removed. Then the Iolite software created an expected downhole trend based on the standard's measurements. Sample crystals that departed from this expected fractionation pattern were given higher standard deviations.

All ages and uncertainties given herein were produced using Isoplot for Microsoft Excel. Commiserate with standard practice, crystals with ages over 1,000 Ma are quoted using ^{206}Pb/^{238}U measurements while, crystals younger than 1,000 Ma are quoted using ^{207}Pb/^{206}Pb (Xie et al. 2010, Sniderman 2013). This is meant to account for the lack of radiogenic ^{207}Pb in the older samples. A ±10% discordance threshold was applied to the grain ages with discordance percent equal to $100 \times [1 - \frac{Age(^{206}\text{Pb}/^{238}\text{U})}{Age(^{207}\text{Pb}/^{235}\text{U})}]$. This is intended to screen out potentially compromised samples that might return unreliable minimum ages. The ^{206}Pb/^{238}U to ^{207}Pb/^{235}U discordance measure is more stable than a ^{206}Pb/^{238}U to ^{207}Pb/^{206}Pb discordance threshold because the measurement of ^{235}U is less affected by quantization noise compared to ^{207}Pb/^{206}Pb (written communication with Mark Brandon and Jeremy Hourigan). It should be noted that when calculating minimum ages all grains were included regardless of discordance because the young grains

had lower Uranium and thus do not contain enough radiogenic ^{207}Pb to produce a precise $^{207}Pb/^{206}Pb$ age. However crystals with large uncertainties are weighted less in the minimum age MATLAB script, so even if a crystal is highly discordant its influence on the minimum age was small (written communication with Mark Brandon and Jeremy Hourigan).

4.2 Vitrinite Reflectance Samples:

120 vitrinite reflectance measurements come from Park Snavely at the USGS. 100 samples have previously been featured in Kvenvolden et al. 1989, a USGS Bulletin that looked at the western Olympics as a potential hydrocarbon source, while the remaining 20 samples are unpublished and focus on the eastern Olympics (Kvenvolden et al. 1989). Mark Brandon proofed the previously unpublished measurements July 12, 2001.

Maximum temperature calculations from the vitrinite reflectance data are based on a linear reduction model from in Barker and Pawlewicz 1994 constructed from reflectance data from 72 depositional settings (Barker and Pawlewicz 1994). Mean random vitrinite reflectance and maximum temperature are strongly correlated because vitrinite reflectivity is dependent on multiple chemical reactions whose activation energy when taken in aggregate is relatively smooth because when one reaction finishes another starts (Sweeney and Burnham 1990). Temperature maximum was calculated by: $\ln(\%R_m) = 0.0124\,T_{\max} - 1.68$ (Barker and Pawlewicz 1994). It should be noted that Sweeney and Burnham 1990 suggest the use of a multi-phase Arrhenius reduction technique, however this method requires reliable zircon or apatite FT lengths. It is our opinion that variable structural integrity of the zircon or apatite crystals induces significant variability, and for regional scale analysis the Barker and Pawlewicz linear reduction is sufficient.

4.3 Fission Track Zircon Samples:

The Fission Track zircon minimum ages have been compiled from published works by Mark Brandon and others (Brandon and Vance 1992, Stewart and Brandon 2004). As previously stated, efforts to date the sedimentary assemblages

of the OSC has relied on fission-track zircon ages and in the original fission-track zircon analysis the authors determined if the zircons in each sample were depositional, partially thermally reset, or thermally reset (Brandon and Vance 1992, Stewart and Brandon 2004). Herein will refer to both the partially thermally reset and the thermally reset samples simply as reset.

5. Results:

5.1 U/Pb Zircon:

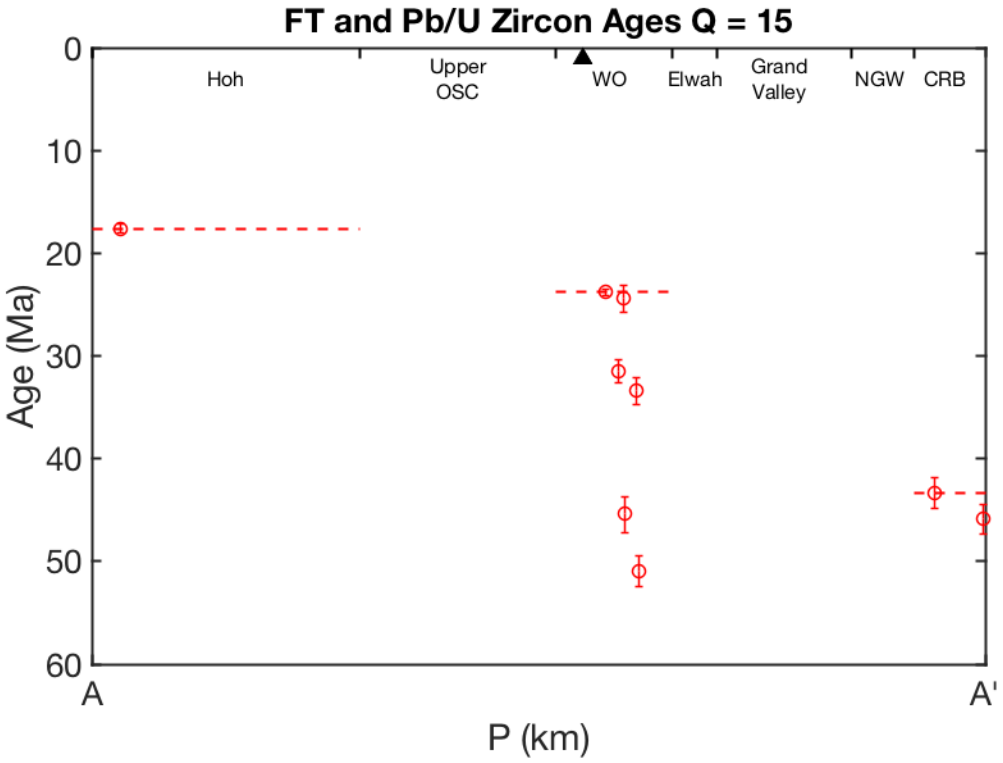

Figure 3: U/Pb zircon ages (red circles); A-A' based on a cross-section from figure 1. Samples further than ± 15 km from A-A' were excluded.

The U/Pb minimum ages appear to get older from west to east. The youngest sample, 170810-1 was collected in the Hoh formation and has a minimum age of 17.6 Ma. Moving deeper into the wedge formation along the A-A' cross-section the minimum ages get older and more diverse around Mount Olympus. The youngest minimum age in the Western Olympic lithic assemblage was from sample 170825-1 collected at the summit of Mount Olympus and records a depositional age of 23.8

Ma. The oldest minimum age in the Western Olympic lithic assemblage is from sample 170823-5 collected at the Hoh River Bridge and records a minimum age of 51 Ma, more than twice the minimum age from the summit. The furthest east samples in the Needles-Gray Wolf and Coastal Range Basalt regions are over 40 Ma and do not exhibit the same variability as the samples near Mount Olympus.

We consider the U/Pb grain ages for the Mahony/Brandon samples to be reliable because the samples contained very few discordant grains and the discordant grains appear to be random. While the minimum age calculation factors in grain discordance into the standard error, samples with a high number of discordant grain ages are not reliable because discordance is often correlated with radiation damage, crystal size, or Uranium content; variables that can be influenced by the age and/or formation of the crystal (Gehrels 2012). If a high percentage of discordant grains are removed from a sample dataset then the remaining non-discordant ages will strongly influence the minimum age calculation, resulting in a minimum age that is not indicative of the full suite of zircons in the sample (Gehrels et al. 2008, summarized in Gehrels 2012). On average only ~2% of the grain ages exceeded the ±10% discordance threshold. Sample 170823-4, collected north of Elk Lake in the Western Olympic lithic assemblage had the highest percentage of discordant grains at ~5%, but this should not significantly effect the minimum age calculation. The lack of discordant grains suggests that the formation processes and the accretionary system did not preferentially preserve certain zircon ages.

Two of the samples tested by U/Pb dating record abnormally old minimum ages. Sample 170823-1 collected at the base of Mount Mathias next to the Blue glacier and sample 170823-5 collected at the southern end of the Hoh River Bridge record minimum ages of 45.4 Ma and 51 Ma respectively. Both of these samples were collected in the Western Olympic lithic assemblage, which is thought to be composed of sediments that were deposited in the trench and accreted to the wedge (Brandon and Vance 1992). There are two possible explanations for these old minimum ages: one, these samples represent a previously undated remnant of the structural lid that is similar in age to the Needles-Gray Wolf assemblage or two, that none of the young zircons that were present in the sample were dated. Considering

that ~100 grains per sample were tested and ~15% of the grain were from the Cenozoic it is possible that samples 170823-1 and 170823-5 contained young grains but they were not tested, and thus the minimum age calculation returned a non-diagnostically old depositional age. The second option is our preferred interpretation considering that an unreset fission track zircon sample ~200 m southeast of sample 170823-5 recorded a minimum age of only 26.5 Ma, suggesting that there isn't a large section of structural lid in the vicinity (Brandon and Stewart 2004). To determine whether the minimum ages of 170823-1 and 170823-5 are indicative of a new formation or simply a byproduct of sampling error an additional 100 zircons per sample will be dated. By testing more grain ages we hope to limit sampling error and increase the probability of dating any young grains that are present in the samples.

5.2 Vitrinite Reflectance:

The vitrinite reflectance temperatures are lower to the west and get hotter to the east and are independently verified by reset fission-track zircons (figure 4). Vitrinite samples collected in the coastal areas of the Hoh lithic assemblage record low maximum temperatures of between 100°C and 200°C or ~5-10 km depth based on a 20°C/km thermal gradient (Brandon and Vance 1992). The vitrinite samples collected in the Western Olympic, Elwah, and the eastern portion of the Grand Valley assemblages record temperatures of ~250°C, which would suggest a depth of 12.5 km. Yet further east the sediments did not reach as high of temperatures. The western portion of the Grand Valley assemblage reached a thermal maximum of 200 - 250°C and samples from the Needles-Gray Wolf span from >200°C at the western

margin to ~125 °C, near the Hurricane Ridge fault.

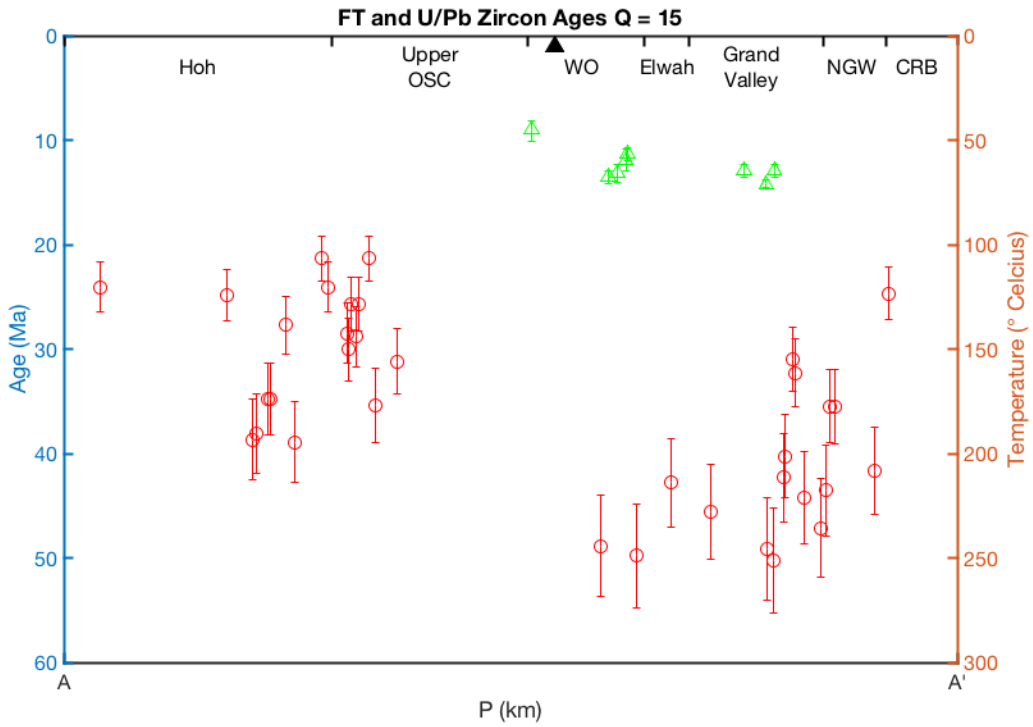

Figure 4: Reset fission track zircon ages (green triangles; left axis), Vitrinite reflectance maximum temperatures ±10% (red circles; right axis)

The vitrinite reflectance data is corroborated by the occurrence of thermally reset fission tracks in zircons. Reset fission-track samples are located in the Western Olympic and Grand Valley assemblages indicating that these rocks reached higher temperatures than the fission-track samples in the other lithic assemblages that were not reset (figure 4). Fission tracks in zircons begin to anneal above ~200°C and fully anneal by ~245°C, so the presence of thermally reset fission-track samples in sites that vitrinite reflectance analysis suggests reached ~250°C is to be expected (Brandon and Vance 1992). The thermally reset fission-track ages and vitrinite thermal maximum temperatures come from different crystal systems and have different modes of recording temperature, this means that a confounding variable in the vitrinite system is unlikely to affect the zircon system and vice versa. We therefore use the reset fission-track samples to independently verify our vitrinite reflectance maximum temperatures as they are related only by maximum temperature. Both datasets broadly show that the eastern assemblages were

warmer, and more specifically that the Western Olympic and Grand Valley assemblages were >250°C. We therefore conclude that our vitrinite reflectance maximum temperature approximations are reliable and offer a decent regional approximation of the maximum thermal temperatures.

6. Discussion:

To analyze the ages of the different lithic assemblages in the OSC we propose that the youngest sample in a contiguous lithic body is an approximation of the age of deposition for the entire assemblage. This is a corollary of the Stewart and Brandon 2004 concept that young grain ages are a proxy for the depositional age of a sample and expands the idea to consider that the minimum sample age in a structural unit is a proxy for depositional age of the entire unit (Stewart and Brandon 2004). This method offers a generalized look at the relative depositional ages of the different sedimentary packets across the accretionary prism.

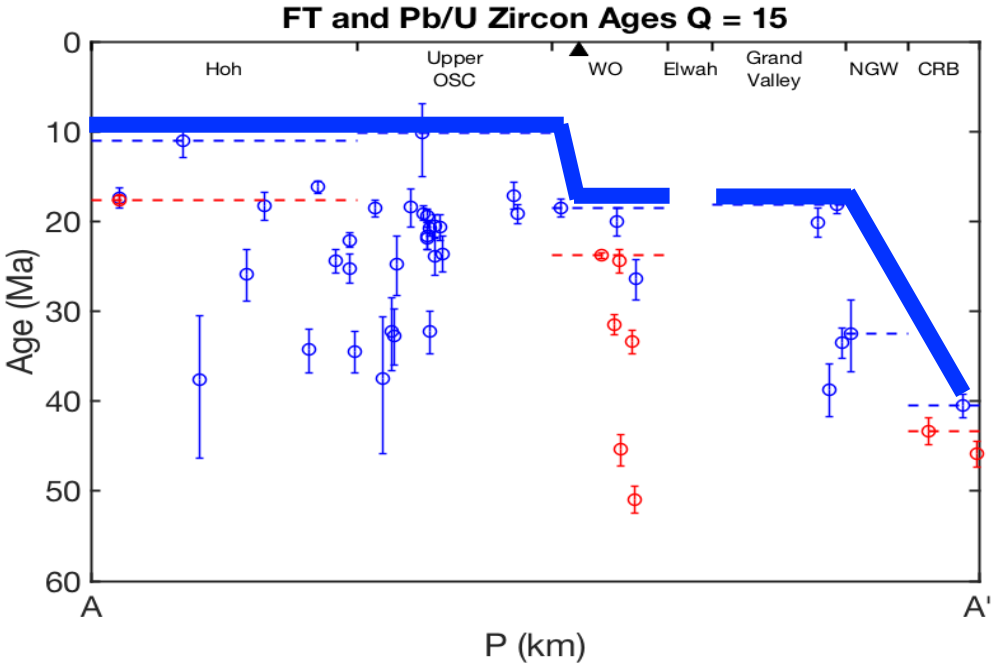

Figure 5: Unreset fission-track zircon minimum ages (blue circles), U/Pb zircon minimum ages (red circles). The implied depositional age of the lithic assemblages are denoted by dashed lines based on the dataset. The implied depositional ages from the fission-track zircon data set (blue dashed lines) are younger than those from the laser ablated U/Pb dataset (red dashed lines) likely because the U/Pb system is less influenced by partial thermal resetting. The implied depositional age

based on a combined dataset of the fission track and laser ablated zircon ages is marked by the bold blue line.

The new U/Pb and the published fission-track minimum ages indicate that the sedimentary blocks exposed in the eastern portion of the Olympic Mountains are older than those exposed in the western portion. The U/Pb and unreset fission-track ages both indicate that there is a general east to west younging with the U/Pb depositional ages being slightly older. Figure 5 shows that the Coastal OSC (Hoh lithic assemblage) and the western portion of the Upper OSC were deposited around the same time ~10 Ma, the Lower OSC (Western Olympic and Grand Valley lithic assemblages) were deposited ~18 Ma, and the structural lid contains the oldest units with the Needles-Gray Wolf at ~32.5 Ma and the Coastal Range Basalts at ~40.5 Ma.

It should be noted that Brandon and Vance 1992 suggest that the western extent of the Upper OSC is closer in age to the Upper OSC units east of Mount Olympus, however our cross-section suggests that the western extent of the Lower OSC is more similar to the Coastal OSC. This discrepancy is likely because the location of the sedimentary units and fault lines in the Western Olympics is not as well defined as the eastern units and it is possible that the we have assumed different constraints for the western assemblages (Tabor and Cady 1978b). It is also possible that samples north of the cross section, in the portion of the Hoh formation that projects eastward, are erroneously labeled as Western Upper OSC based on their distance from the Kalaloch Lodge (point A). However the youngest sample labeled as part of the Lower OSC, which is used to determine the depositional age, is located south of the cross section and is therefore not part of the eastern projection of the Hoh. While additional mapping of the Western Olympics would be necessary to further constrain the location of the different underlying sedimentary packets, creating a high fidelity geologic map would be difficult considering much of the region is covered by quaternary sediments eroded from the central massif.

The presence of older sediments to the east of the range is consistent with current wedge theory, which suggest that the wedge has progressively built out westward (summarized in Brandon 2004). As more sediment has been added at the

margin the older sediments are pushed deeper into the wedge. As you travel from the Hurricane Ridge fault to the coast you move down the accretionary wedge with the earliest accreted units abutting the Coast Range terrane and the newest sediments presently entraining at the deformation front (Brandon 2004). The Upper OSC would have been the first sedimentary lithic assemblage accreted during early wedge formation when it was thrust beneath the Coastal Range Terrane, then the marine sediments that make up the Lower OSC were incised and projected beneath the Upper OSC, and the newest sedimentary structures exposed nears the coast were added at the deformational front (Brandon and Vance 1992).

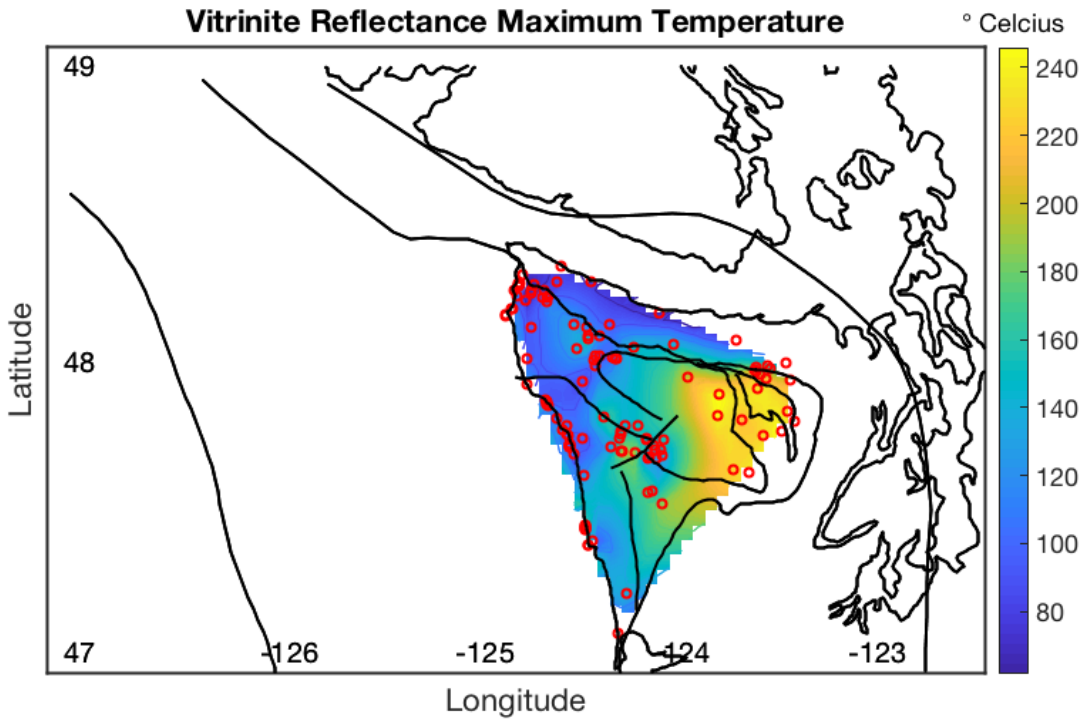

Figure 6: Maximum temperatures calculated from vitrinite reflectance $\%R_m$ using a linear calibration by Barker and Pawlewicz 1994 for vitrinite in depositional environments. Vitrinite reflectance samples (locations marked by red circles) were collected by Park Snavely, USGS.

The eastern sedimentary units of the Olympic Subduction Complex also record thermal maximums higher than coastal and peripheral regions. In a similar fashion as the depositional ages, the maximum temperatures show a regional east to west gradient, and once again this is consistent with current wedge theory. When

the Upper OSC unit was incised and plunged beneath the coastal range terrane it was transported from the surface, where temperatures are mild, to depths consistent with temperatures exceeding 200°C or about 10 km (Batt et al. 2001). The Lower OSC experienced similar incision and burial and exhibit high thermal maximums consistent with deep burial (Batt et al. 2001). The costal regions however were likely never deeply buried as they formed by accreting on the front edge of the wedge and have not been subaerially exposed long enough to result in significant erosion induced exhumation (Batt et al. 2001). The samples on the periphery are outside the sedimentary core were likely sampled from sedimentary formations atop the Coastal Range terrane. These Coastal Range samples record low temperatures ~80°C because they have never had a significant layer overtop of them.

The samples were exhumed by surface erosion because as material was removed from the surface the subterranean sediments were able to rise to take their place, as new material from the subducting plate created uplift (Pazzaglia and Brandon 2001 Brandon et al. 1998). This process of surface removal and uplift has resulted in units that were once deeply buried now being present at the surface. The areas in the Olympic Mountains with the highest elevation have generally experienced the highest rates of erosion (Batt et al. 2001, Montgomery and Brandon 2004, Ehlers 2018). The Upper OSC and Lower OSC in the eastern portion of the system are at the high divide of the Olympic Mountain Range, so we would expect them to have experienced the most erosion and as a result the most exhumation (Montgomery and Brandon 2004, Ehlers 2018). This is verified in the vitrinite thermal data, because east of Mount Olympus the vitrinite samples consistently record maximum temperatures between 200-250°C (10-12.5 km). The maximum temperature data implies that at one point there was 10 to 12.5 kilometers of sedimentary cover above the presently exposed eastern units, however the cover has since eroded allowing the deep sediments to rise to the surface.

One complication in the vitrinite maximum temperature dataset is that the maximum temperatures of the Elwah Unit in the Upper OSC record temperatures similar to that of the Lower OSC. If the Upper OSC is part of the structural lid, as

postulated by Brandon and Vance 1992, then we would expect it to exhibit lower temperature maximum readings compared to the deeper Lower OSC (Brandon and Vance 1992). However, because the Elwah assemblage is between two Lower OSC units, the Grand Valley and the Western Olympic assemblages, it is possible that the Elwah was conductively heated by its proximity to the rising Lower OSC units that retained some heat during exhumation. This conductive heating effect of the Lower OSC to the Upper OSC can be seen in figure 4 as the maximum temperatures in the Needles Gray Wolf assemblage is highest on the margin with the Grand Valley assemblage, but the maximum temperatures decrease towards the Hurricane Ridge ultimately recording temperatures similar to the shallow coastal units.

7. Summary:

The Olympic Mountains in Washington represent the exposed accretionary wedge of the Cascadia subduction zone that formed as sediments from the subducting Farralon and Juan de Fuca plate accreted to the overriding North American continent. Subduction began ~35 Ma and currently spans from northern California to southern British Columbia (Vance et al. 1986, summarized in Brandon and Vance 1992). The Olympic Subduction Zone can be used as an analog for general subduction related wedge formation to show that sediments generally build outwards from the continental plate.

Using unrest fission-track zircon and laser-ablated U/Pb zircon ages we have approximated the depositional age of the sedimentary lithic assemblages in the Olympic Subduction Complex. By considering the youngest grains in a sample to be indicative of the depositional age of the entire lithic assemblage we were able to show that the accreted sediments furthest from the accretionary front were the first to be entrained to the continent and subsequent sedimentary layers built out away from the continent.

Additionally, we have analyzed reset fission-track zircon samples and vitrinite reflectance measurements to conclude that the eastern portion of the Olympic Mountains reached a higher maximum temperature during accretion than the more coastward units. This suggests that units presently exposed in the eastern

portion of the Olympic mountains are the most exhumed sediments and that at one point during accretion these units were plunged to depths of ~12.5 km. Our findings are commiserate with current wedge theory from Brandon and Vance 1992 that suggests that Olympic Subduction Complex build out eastward from the North American continent with the Upper OSC thrust beneath the Coastal Range terrane, the Lower OSC beneath the Upper OSC, and the Coastal OSC remaining near the surface.

8. Acknowledgements:

I would like to thank my thesis advisor, Mark Brandon, for his enthusiasm and guidance. From discussing roadside geology in Washington to editing rough drafts at Yale you made the process engaging and stimulating. Jeremy Hourigan and his team at University of California, Santa Cruz were integral to acquiring the LA-ICP-MS data and I'd especially to thank Dr. Hourigan for teaching me the basics of isotope data reduction. I would also like to thank Parker D. Snavley and Richard J. Stewart; although we never met, the samples and data that you collected were essential to this project. The financial backing offered by the Yale Department of Geology and Geophysics by the Van Dam Research Fellowship helped make this project possible. Lastly, I would like to thank my younger brother Glen Mahony and my childhood friend Charlie Reinertson for helping me carry samples (aka rocks) out of the park. It was an unforgettable trip and I'm sorry that I forgot to mention that our bags would be heavier on the hike out than on the hike in.

9. Appendix:

U/Pb Samples Collected by Mahony and Brandon:

170810-1:

This sample was a thick-bedded, medium-grain overturned sandstone from the Hoh assemblage, collected from Beach 3 north of Kalaloch. 103 detrital zircon grains were analyzed, and 2 triggered the ±10% discordance threshold. The minimum age of the sample is 17.6 Ma.

170811-1:

This sample was medium-bedded, medium-grain sandstone with laminated shale interbeds from the Hoh assemblage, collected north of Highway 2750, east of Mt. Octopus. 102 detrital zircon grains were analyzed, and 4 triggered the ±10% discordance threshold. The minimum age of the sample is 19.2 Ma.

170811-2:

This sample was a massive medium-grain sandstone from the Western Olympic assemblage, collected next to Calawah River on Sitkum-Sol Duc Road. 100 detrital zircon grains were analyzed, and 0 triggered the ±10% discordance threshold. The minimum age is 47.4 Ma.

170811-3:

This sample was a bedded sandstone from the Needles-Gray Wolf assemblage, collected on Hurricane Hill, west of Hurricane Ridge Visitor Center. 100 detrital zircon grains were analyzed, and 2 triggered the ±10% discordance threshold. The minimum age is 36.9 Ma.

170812-1:

This sample was thin-bedded turbidite sandstone with mudstone interbeds from the Blue Mountain Unit, collected south of the summit of Blue Mountain. 100 detrital zircon grains were analyzed, and 1 triggered the ±10% discordance threshold. The minimum age is 43.3 Ma.

170812-2:

This sample was a thin-bedded sandstone and mudstone from the Blue Mountain unit, collected north of Gray Wolf River on Forest Service road 2860. 100

detrital zircon grains were analyzed, and 0 triggered the ±10% discordance threshold. The minimum age is 45.9 Ma.

170812-3:

This sample was medium-bedded sandstone and mudstone from the Blue Mountain unit close to sample 170812-2 but includes thicker and coarser sandstone beds. 100 detrital zircon grains were analyzed, and 1 triggered the ±10% discordance threshold. The minimum age is 45.9 Ma.

170816-1:

This sample was a sandstone, from the Elwha assemblage, collected from the Enchanted Valley cliff wall. 100 detrital zircon grains were analyzed, and 2 triggered the ±10% discordance threshold. The minimum age is 33 Ma.

170816-2:

This sample was a sandstone, from the Elwha assemblage, collected at Anderson Pass. 97 detrital zircon grains were analyzed, and 4 triggered the ±10% discordance threshold. The minimum age is 32.1 Ma.

170816-3:

This sample was a sandstone, from the Elwha assemblage, collected at the south end of the Anderson Glacier tarn. 102 detrital zircon grains were analyzed, and 3 triggered the ±10% discordance threshold. The minimum age is 28.5 Ma.

170823-1:

This sample was a sandstone, from the Western Olympic assemblage, collected at the base of Mount Mathias north of the Blue Glacier and Mount Olympus. 101 detrital zircon grains were analyzed, and 2 triggered the ±10% discordance threshold. The minimum age is 45.4 Ma.

170823-2:

This sample was a sandstone, from the Western Olympic assemblage, collected at terminal moraine of the Blue Glacier as denoted by trail signs posted by the US National Parks Service. 101 detrital zircon grains were analyzed, and 0 triggered the ±10% discordance threshold. The minimum age is 31.5 Ma.

170823-3:

This sample was a sandstone, from the Western Olympic assemblage, collected at the ~200 m downslope from the base of the Glacier Meadows ladder. 100 detrital zircon grains were analyzed, and 4 triggered the ±10% discordance threshold. The minimum age is 24.4 Ma.

170823-4:

This sample was a sandstone, from the Western Olympic assemblage, collected north of Elk Lake ~10 m upslope from the Hoh trail. 101 detrital zircon grains were analyzed, and 5 triggered the ±10% discordance threshold. The minimum age is 33.4 Ma.

170823-5:

This sample was a sandstone, from the Western Olympic assemblage, collected at the southern anchor point for the Hoh bridge. 100 detrital zircon grains were analyzed, and 3 triggered the ±10% discordance threshold. The minimum age is 51 Ma.

170825-1:

This sample was a large-grain, thick-bedded sandstone from the Western Olympic assemblage, collected at the summit of Mount Olympus by the construction crew that built the SC03 GPS in 2002. From the sample 74 detrital zircon grains were analyzed, and 1 triggered the ±10% discordance threshold. The minimum age is 23.8 Ma.

When writing this paper I found it helpful to review and summarize the literature as I went, however several important topics did not fit the scope of the final product and I have decided to include them here.

Thickening:

Brandon's interpretation of the OSC is contingent on both significant uplift of the coastal range terrane and erosion to exhume the Coast Range basalt and Upper OSC. The development and scale of a wedge is contingent on the rate of incoming material from the trench and the rate of outflowing material from erosion (Willet et al. 2001, Willet and Brandon 2002). In the case of the OSC the Juan de Fuca plate is

subducting beneath the North American plate at a rate of 32 km/Ma and if all of the incoming sediments are entrained and compressed by a factor of 65% that would result in a cross-sectional volume influx of ~52 km^2/Ma into the wedge (Brandon 2004). Based on current wedge taper and cross sectional area it would take 70 Ma to build the OSC, which is longer than the 36 Ma of subduction (Brandon 2004). For this reason fission track cooling ages are instead used to constrain the average rate of thickening to 0.6 km/Ma from 36 Ma to 17 Ma and 1.75 km/Ma from 17 Ma to present (Brandon and Calderwood 1990, Brandon and Vance 1992). Using these figures it would suggest a total vertical thickening of >40 km over the lifetime of the subjection zone. Lithoprobe seismic reflectance data of the peninsula suggests that the accretionary prism is composed almost entirely of metamorphosed sediments and is ~30 km thick (Clowes and Brandon 1986). This suggests the accumulation of sediments at the continental margin was sufficient to uplift the structural lid via Austroalpine-scale regional folding to produce a nappe like-structure, which erosion then removed the top ~10 km exposing the wedge prism and the inclined coastal range terrane (Summarized in Brandon 2004, Brandon and Calderwood 1990).

Erosion:

Erosion in tectonically active hill slopes is correlated with local precipitation rates. The Olympic core is the topographic high of the peninsula with the Seattle Basin to the East, the continental margin to the West, the Tofino Basin stretching from western Vancouver Island into and Straight of Juan de Fuca to the north, and the Wallipa-Grays and Harbor Basins to the South (Tabor and Cady 1978a). The forearc high is located at Mount Olympus approximately 60 km west of the Seattle Basin and 200 km east of the deformation front at the convergent margin and this aerially exposed terrain influences local weather and produces a drastic windward and leeward precipitation differential (Ehlers 2018). Moist air from the Pacific Ocean drops 5,000 to 6,000 mm/year of precipitation on the western side of the Peninsula as compared to 1,000 to 2,000 mm/year east of Mount Olympus (Ehlers 2018). The heavy rains on the western side of the mountain range create the conditions for both the lush ecosystem of the Hoh Rainforest and significant erosion.

The high precipitation rates and glacial history of the OSC cause highly concentrated erosion on the Mount Olympus massif. The drainage system of the western side of the range, including the Hoh, Queets, and Quinault rivers, trace deeply incised Pleistocene alpine glacier valleys from the range's interior (Ehlers 2018). The Hoh river watershed flows through both logged and virgin terrain in the northwest of the Olympic Mountains and erodes an estimated .32 km/Ma (Nelson 1986). The only significant northward drainage is the Elwha River that has headwaters at the base of Mount Queets and drains through natural forestland into the straight of Juan de Fuca west of Port Angeles. Research involved in dam removals along the Elwha River suggests rivers in native Olympic forestland have a sediment yield between .11 km/Ma and .18 km/Ma (Stoker and Williams 1991). Eastern draining rivers, like the Ducabush, Docewallups, and Quilcene, are considerably smaller than the Elwha and Hoh, but still contribute to the total sediment erosion of the mountain range. By integrating a contour of Apatite thermal closure ages Brandon estimates the average erosion rate of the Olympic Mountains is ~.28 km/Ma with the most intense erosion (0.75 km/Ma) concentrated near Mount Olympus (Brandon et al. 1998). That the highest rate of erosion is centered at Mount Olympus, an area known for orographic precipitation and deeply incised glacier valleys, agrees with the current theory that erosion rates of tectonically active slopes is highly dependent on mean local relief (Montgomery and Brandon 2002) and precipitation (Willet 1999). The erosion rate of ~.28 km/Ma is also within the range of the Elwha and Hoh sedimentation rates (Brandon et al.1998) suggesting that most of the eroded sediments are removed from the Olympic interior by the river systems. These fluvial sediments are ultimately deposited on the Cascadia Abyssal Plane, either directly or after a brief residence in the Puget Sound before being transported through the Strait of Juan de Fuca (Brandon et al. 1998). It should be noted that recent findings in (Ehlers 2018) suggest slightly higher rates of erosion from a low of .25 km/Ma to a high of .9 km/Ma with the highest rates of erosion still focused on the central massif.

Erosion rates appear to have reached a steady state nearly 14 Ma ago (Brandon et al. 1998, Pazzaglia and Brandon 2001, Ehlers 2018). By analyzing the

sinuosity of westward draining rivers relative to flat bedrock terraces Pazzaglia and Brandon suggest that the incision and erosion rates of rivers in the Olympic Mountains have been relatively constant for the last ~100 ka, but can be highly variable on shorter time scales due to periods of glaciation (Pazzaglia and Brandon 2001). The dependence on the interglacial cycle matches fission track findings from Ehlers, which required significantly higher erosional rates starting 2 to 3 Ma during the Pleistocene glaciation (Ehlers 2018). Additional fission track data from Brandon suggest that erosion rates have been broadly consistent for the last 7 Ma, and zircon cooling ages from the central massif suggest the erosion rates there have remained constant for the last 14 Ma (Brandon et al. 1998). If exhumation began 14 Ma and maintained present rates 10.5 to 12.5 km have been removed from atop the OSC interior, this would be sufficient to remove the structural lid to expose the previously buried accretionary prism and a heavily inclined coastal range terrane (Brandon 2004).

Vitrinite Measurements:

Vitrinite reflectance is commonly used to constrain the maximum temperature of humic organic materials. Vitrinite is a metamorphic product formed when the woody tissue of plants is thermally cooked. In both laboratory and geological conditions it has been shown that the ratio of incoming light to reflected light, known as vitrinite reflectance ($\%R_0$), is highly correlated with the maximum temperature of exposure (summarized in Sweeney and Burnham 1990). The oil and gas industry pioneered vitrinite reflectance analysis as a method for measuring the thermal maturity of downhole sediments in order to pinpoint the ideal drilling depth in a reserve, referred to as the oil window (Hunt 1979, and many others, summarized in Sweeney and Burnham 1990 and Barker and Pawlewicz 1986). Vitrinite reflectance has also been used to determine the thermal maturity of sediments near intrusions and in depositional environments (Barker et al. 1986, Barker 1989, summarized in Sweeney and Burnham 1990).

The vitrinite reflectance ($\%R_0$) was determined using best practices outlined by the American Standards for Testing Materials (ASTM D7708). For each sample a

thin section was made and analyzed under 500x magnification in oil immersion by a microscope equipped with a sensitive photometric device. The microscope stage was leveled and the aperture focused to limit glare. The vitrinite in the sample was then identified using standard petrography techniques and the stage adjusted so the photometer was trained on the mineral. The illumination aperture was then closed and with no light reflecting off the sample the photometer was set to zero, accounting for dark current bias based on the device specifications. To calibrate the system the vitrinite was exposed to white light and the photometer readout recorded; without changing the settings the stage was adjusted to focus on a series of standards with similar reflectance's and the values recorded. The system was calibrated so that the standard's reflectance was within 0.001% of published values. Then, using non-polarized white light, the reflectance of non-pitted but otherwise random samples of vitrinite was recorded. Once 20-30 randomized measurements were obtained a $\%R_0$ probability density plot is created. Unless otherwise stated, the vitrinite reflectance values given herein are mean random vitrinite reflectance ($\%R_m$), where $\%R_m$ and associated standard errors are that of the $\%R_0$ probability density plots based on 20-30 vitrinite reflectance measurements (summary of vitrinite reflectance methodology based extensively on AMTM D7708).

Works Cited:

Applegate, J.D.R., and Brandon, M.T. (1989) An upper plate origin for basalt blocks in the Cenozoic subduction complex of the Olympic Mountains, northwest Washington State. Geological Society of America, Abstracts with Programs, **21**: 51.

Armstrong, R.L., (1978) Cenozoic igneous s history of the US Cordillera from lat. 42 to 49N. *GSA Memoir* **152**: 265-282.

Armstrong, R.L., (1986) Lab Procedures for Mineral Seperation at University of British Columbia.

ASTM D7708. Standard Test Method for Microscopical Determination of Vitrinite Dispersed in Sedimentary Rocks. Book of Standards 5.06.

Barker, C.E., (1989) Temperature and Time in the Thermal Maturation of Sedimentary Organic Matter. Thermal history of sedimentary basins-methods and case histories: New York, Springer-Verlag, p. 75-98.

Barker, C.E., and Pawlewicz M.J. (1986) The correlation of vitrinite reflectance with maximum temperature in humic organic matter. Paleogeothermics **5**: 79-93.

Barker, C.E., and Pawlewicz M.J. (1994) Calculation of Vitrinite Reflectance from Thermal Histories and Peak Temperatures. ACS Symposium Series: Vitrinite Reflectance as a Maturity Parameter 216-229.

Batt, G.E., Brandon, M.T., Farley, K.A., and Roden-Tice, M., (2001) Tectonic synthesis of the Olympic Mountains segment of the Cascadia wedge, using two-dimensional thermal and kinematic modeling of thermochronological ages. *J. of Geophysical Research* **106**: 26,731-46.

Brandon, M.T., (2004) the Cascadia Subduction Wedge: The role of accretion uplift and erosion. In: "Earth Structure, An Introduction to Structural Geology and Tectonics", by B.A. van der Pluijm and S. Marshak, Second Edition, WCB/McGraw Hill Press, p. 566-574.

Brandon, M.T., Roden-Tice, M.K., and Garver, J.I., (1998) Late Cenozoic exhumation of the Cascadia accretionary wedge in the Olympic Mountains, northwest Washington State. GSA Bulletin **110**: 985-1009.

Brandon, M.T., and Calderwood, A.R., (1990) High-pressure metamorphism and uplift of the subduction complex. *Geology* **18**: 1252-55.

Brandon, M.T., Vance, J.A., (1992) Tectonic Evolution of the Cenozoic Olympic Subduction Complex, Washington State, as deduced from Fission Track ages for Detrital Zircons*. American Journal of Science* **292**: 565-636.

Cherniak, D.J., and Watson, E.B., (2001) Pb diffusion in zircon. *Chemical Geology*. **172**: 5-24.

Clowes, R.M., Brandon, M.T., et al. (1986) Lithoprobe-southern Vancouver Island: Cenozoic subduction complex imaged by deep seismic reflections. *Can. J. Earth Sci.* **24** 31-51.

Ehlers, T.A., Michel, L. et al. (2018) Tectonic and glacial contributions to focused exhumation in the Olympic Mountains, Washington USA. GSA repository 2018161.

Frost, B.R., (1980) Observation on the boundary between zeolite facies and prehnite-pumpellyite facies. *Contributions to Mineralogy and Petrology* **73**: 365-373.

Gehrels, G.E., Valencia, V.A., and Ruiz, J., (2008) Enhanced precision, accuracy, efficiency, and special resolution of U-Pb ages by laser ablation-multicollector inductively coupled plasma-mass spectrometry. *AGU Technical Brief* **9**:3.

Gehrels, G.E., (2012) Detrital zircon U-Pb geochronology: current methods and new opportunities. In 'Tectonics of Sedimentary Basins: Recent Advances, First Edition" by Cathy Busby and Antonio Azor. Blackwell Publishing Ltd.

Heller, P.L., Tabor, R.W., et al. (1987) Isotopic provenance of Paleogene sandstones from the accretionary core of the Olympic Mountains, Washington. *GSA Bulletin* **104**: 140-153.

Hunt, J.M., (1979) Petroleum geochemistry and geology. New York, W.H. Freeman p. 28-339.

Johnson, S.Y., (1984) Evidence for a margin-truncating transcurrent fault (pre-late Eocene in western Washington. *Geology* **12**: 538-541.

Kvenvolden, K.A., Golan-Bac, M., and Snavely, P.D. Jr., (1989) Preliminary evaluation of the petroleum potential of the Tertiary accretionary terrane, west side of the Olympic Peninsula, Washington. *USGS Surv. Bulletin* **1892**: 21-35.

McCaffery, R., King, R.W., Payne, S.J., and Lancaster, M., (2013) Active tectonics of northwestern U.S. inferred from GPS-derived surface velocities. *J. of Geophysical Research: Solid Earth* **118**:2.

Montgomery, D.R., and Brandon, M.T., (2004) Topographic controls on erosion rates in tectonically active mountain ranges. *Earth and Planetary Science Letters* **201**: 481-489.

Monger, J.C., Byrne, T., Plumley, P.W., et al. (1982) Tectonic accretion and the origin of two major metamorphic and plutonic welts in the Canadian Cordillera. *Geology* **10**: 70-75.

Nelson, L.M., (1986) Fluvial sediment in the Hoh River. In " Reconnaissance of the water resources of the Hoh Indian reservation and the Hoh River basin". *USGS Water Resources Investigations Report* WRI-85-4018.

Paton, C., et al. (2010) Improved laser ablation U-Pb zircon geochronology through robust downhole fractionation correction. *Geochem. Geophys. Geosyst*. 11.

Pazzaglia, F.J., and Brandon, M.T., (2001) A Fluvial Record of Long-term steady-state uplift and erosion across the cascadia forearc high, western Washington State. *American Journal of Science* **301**: 385-431.

Rau, W.W., (1964) Foraminifera from the Northern Olympic peninsula, Washington. *Geological Survey Professional Paper* 374-G.

Roden, M.K., Brandon, M.T., and Miller, D.S., (1990) Apatite fission-track thermochronology of the Olympics subduction complex, Washington. *GSA Abstracts with Programs* **22**: 1223-32.

Sherrod, D.R., and Smith, J.G., (1989) Preliminary map of upper Eocene to Holocene volcanic and related rocks of the Cascade Range, Oregon: *United States Geological Survey* Open-File Report 89-14.

Snavley, P.D. Jr., and Macload, N.S., (1974) Yuchats Basalt—An upper Eocene differentiated volcanic sequence in the Oregon Coast Range: *United States Geological Survey Journal of Research* **2**: 395-403.

Stewart, R.J., and Brandon, M.T., (2004) Detrital-zircon fission-track ages for the "Hoh Formation": Implications for late Cenozoic evolution of the Cascadia subduction wedge. *GSA Bulletin* **116**: 60-75.

Sweeney, J.J., and Burnham, A.K., (1990) Evaluation of a Simple Model of Vitrinite Reflectance Based on Chemical Kinetics. *AAPG Bulletin* **74**: 1559-70.

Siberling, N.J., Jones, D.L., Blake, Jr., M.C., and Howell, D.G., (1987) Lithotectonic terrane map of the western conterminous United States: *United States Geological Survey* Miscellaneous Field Studies Map MF-1874-C.

Sniderman, E., (2013) Detrital Zircon Geochronology and Provenance Analysis of Scotland Group Sediments, Barbados. Senior Thesis for fulfillment of Yale University Geology and Geophysics degree.

Stoker, B.A., and Williams, D.T., (1991) Sediment modeling of dam removal alternatives, Elwha River, Washington. In "Hydraulic Engineering".

Tabor, R.W., and Cady, W.M., (1978a) The structure of the Olympic Mountains ,Washington- analysis of a subduction zone: *United States Geological Survey* Professional Paper 1033.

Tabor, R.W., and Cady, W.M., (1978b) Geologic map of the Olympic Peninsula: *United States Geological Survey* Map I-994.

Vance, J.A., Walker, N.W., and Mattinson J.M., (1986) U/Pb ages of early Cascade plutons in Washington State. *Geological Society of America* Abstracts with Programs **18**:2:p 194.

Wells, R.E., and Heller, P.L., (1988) the relative contribution of accretion, shear, and extension to Cenozoic tectonic rotation in the Pacific Northwest. *GSA Bulletin* **100**: 325-38.

Wells, R., Bukry, D., Friedman, R., et al. (2014) Geologic history of Siletzia, a large igneous province in the Oregon and Washington Coast Range: Correlation to the geomagnetic polarity time scale and implication for a long-lived Yellowstone hotspot. *Geosphere*. **10**: 692-719.

Willet, S.D., (1999) Orogeny and orography: The effects of erosion on the structure of mountain belts. *J. of Geophysical Research* **104**: 28957-81.

Willet, S.D., Slingerland, R., and Hovius, N., (2001) Uplift, shortening, and steady state topography in active mountain belts. American J. of Sci. **301**: 455-485.

Willet, S.D., and Brandon, M.T., (2002) On steady states in mountain belts. *Geology* **30**: 175-178.

Xie, X., Mann, P., and Escalona, A., (2010) Regional provenance study of Eocene clastic sedimentary rocks within the South America-Caribbean plate boundary zone using detrital zircon geochronology. *Earth and Planetary Science* **291**: 159-171.